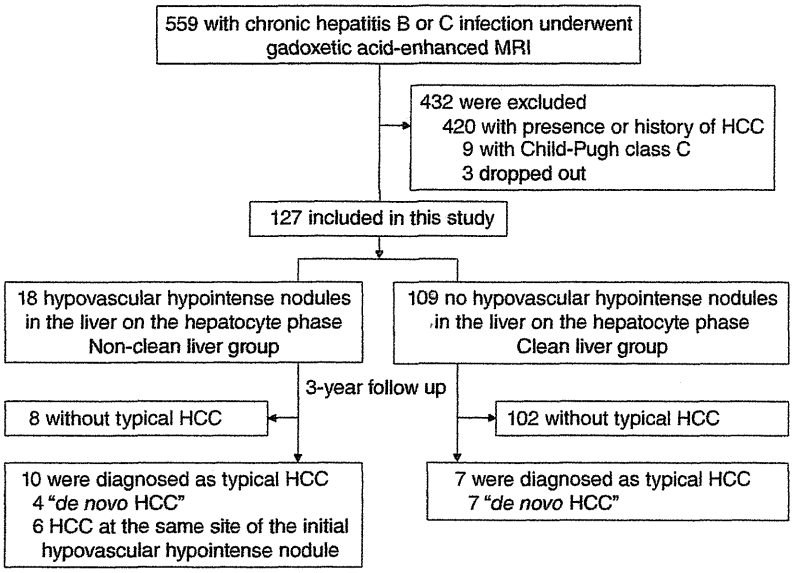

Figure 1 Patient inclusion criteria. "De novo HCC" is a typical hepatocellular carcinoma that developed at sites in which no nodules had been seen on the initial gadoxetic acid-enhanced magnetic resonance imaging (MRI).

modalities led to diagnosis of HCC, recognizing hypervascularization by more than one experienced radiologist and other imaging modalities was regarded as the time of diagnosis of HCC. When needle biopsy was performed to investigate nodules, the time of diagnosis of HCC was when the pathologists and physicians examined pathological tissue and diagnosed as HCC.

MRI

Magnetic resonance imaging was performed using a superconducting magnet that operated at 1.5 Tesla (Sigma EXCITE HD; GE Medical Systems, Milwaukee, WI, USA) and an 8-channel phased-array coil. First, we obtained fast spoiled gradient-echo T_1-weighted images (T1WI) with dual echo acquisition and respiratory-triggered fat-saturated fast spin-echo T_2-weighted images (T2WI). Dynamic fat-suppressed gradient-echo T1WI were obtained using a 3-D acquisition sequence before (precontrast) and 20–30 s, 60 s, 2 min, 5 min, 10 min and 20 min after the administration of gadoxetic acid (Primovist; Bayer Schering Pharma, Berlin, Germany). This contrast agent (0.025 mM/kg bodyweight) was administrated i.v. as a bolus at a rate of 1 mL/s through an i.v. cubital line (20–22 G) that was flushed with 20 mL saline from a power injector. The delay time for the arterial phase scan was adjusted according to a fluoroscopic triggering method.[20] All images were acquired in the transverse plane. Sagittal plane T1WI were also obtained during the hepatocyte phase at 20 min after the injection of the contrast agent.

Statistical analysis

All continuous values are expressed as median (range). Fisher's exact probability test was used for comparisons between categorical variable and the non-parametric Mann-Whitney *U*-test was used to compare differences between continuous variables. Baseline clinical characteristics, including blood test results, were evaluated within 1 month of the initial MRI. We investigated whether or not HCC development was associated with age, sex, fibrosis, etiology (HBV or HCV), platelet count, serum alanine aminotransferase (ALT), γ-glutamyltransferase (γ-GT), α-fetoprotein (AFP), and the presence or absence of hypovascular hypointense nodules.

Cumulative HCC development was estimated according to the Kaplan–Meier method and differences in the curves were tested using the log–rank test. Risk factors for HCC development were determined according to the Cox proportional hazard model. Subgroup analyses with a Cox proportional hazard model were applied to estimation of the hazard ratio (HR) of the non-clean liver group versus clean liver group in the dichotomized subgroups. All statistical analyses were performed using JMP software, version 10 (SAS Institute Japan, Tokyo, Japan). A two-sided *P*-value of less than 0.05 was considered statistically significant.

RESULTS

Characteristics of the patients and nodules

A TOTAL OF 127 patients were enrolled, of whom 26 had chronic HBV infections and 101 had HCV infections, and 68 had virus-associated cirrhosis. No statistically significant differences in the initial clinical characteristics were found between the non-clean liver and clean liver groups (Table 1). Thirty-five hypovascular hypointense nodules were found in 18 patients in the non-clean liver group (1–5 nodules per patient) at baseline (data not shown). Twenty-four of these 35 nodules were detectable only on the hepatocyte phase MRI and were undetectable by US, CT and non-hepatocyte phase MRI. None of the 35 nodules showed high intensity on T2WI. The median nodule diameter was 8 mm (range, 4–13 mm; 33 nodules with ≤10 mm, two nodules with 12 mm and 13 mm).

HCC incidence according to initial MRI findings

Hepatocellular carcinoma was diagnosed in 17 patients, 10 in the non-clean liver group and seven in the clean liver group; 14 of these patients had HCV infection. Thirteen patients were diagnosed according to the AASLD imaging criteria.[19] Four patients were diagnosed pathologically by liver biopsies that were performed, based on enlargement of the nodules of more than 10 mm in diameter during the observation period.

The cumulative 1-, 2- and 3-year HCC incidence rates were 1.5%, 10.2% and 13.4%, respectively. As determined by the Kaplan–Meier method, these rates were 11.1% (95% confidence interval [CI], 0.0–25.6%), 38.8% (95% CI, 16.3–61.4%) and 55.5% (95% CI, 32.6–78.5%) in the non-clean liver group, and 0.0% (95% CI, 0.0–2.3%), 5.5% (95% CI, 0.0–9.8%) and 6.4% (95% CI, 1.8–11.0%) in the clean liver group; the former group showed significantly higher rates of development of typical HCC than the latter ($P < 0.001$) as shown in Figure 2. The median imaging intervals were 3 months (range, 3–6) in the non-clean liver group and 4 months (range, 2–12) in the clean liver group. The imaging interval of the non-clean liver group was shorter than the clean liver group (3 vs 4 months, $P = 0.015$). The median intervals between the initial MRI and HCC diagnosis was 16 months (range, 9–32) in the non-clean liver group and 21 months (range, 16–35) in the clean liver group.

In 11 of 17 patients with HCC development, HCC developed at sites in which no nodules had been seen on the initial gadoxetic acid-enhanced MRI, namely de novo HCC. These HCC were found in four of 18 patients in the non-clean liver group (3-year HCC incidence rates: 22.2%; 95% CI, 4.3–51.0%) and 7 in 109 patients in the clean liver group (3-year HCC incidence rates: 6.4%; 95% CI, 1.8–11.0%). The incidence rates of de novo HCC was significantly higher in the non-clean liver group than the clean liver group ($P = 0.003$, Fig. 3). In the remaining six patients, HCC developed at the same site of the initial nodules exclusively in 18 patients of a non-clean liver group by definition, and those HCC arose among the nodules of 8 mm or more in the initial MRI study.

Risk factors for HCC development

Univariate analyses showed that the significant risk factors for HCC development included older age ($P = 0.039$), cirrhosis ($P = 0.009$), a low platelet count ($P = 0.003$), a high AFP concentration ($P = 0.006$) and a non-clean liver ($P < 0.001$). Multivariate analysis with these variables revealed that older age (hazard ratio [HR], 1.08; 95% CI, 1.01–1.16; $P = 0.024$), a low plate-

Table 1 Baseline patient characteristics

Characteristics	Total ($n = 127$)	Non-clean liver ($n = 18$)	Clean liver ($n = 109$)	P
Age, years	65 (30–88)	68 (46–82)	64 (30–88)	0.15
Male/female	68/59	10/8	58/51	1.00
Non-cirrhosis/cirrhosis	59/68	6/12	53/56	0.31
HBV/HCV	26/101	5/13	21/88	0.53
Platelet count ($\times 10^9$/L)	122 (30–410)	102 (46–187)	125 (30–410)	0.07
ALT (IU/L)	32 (7–206)	32 (14–95)	32 (7–206)	0.97
γ-GT (IU/L)	31 (9–305)	31 (13–258)	31 (9–305)	0.68
AFP (ng/mL)	4 (1–582)	8 (2–181)	4 (1–582)	0.19

Continuous data are shown as medians (range).
γ-GT, γ-glutamyltransferase; AFP, α-fetoprotein; ALT, alanine aminotransferase; HBV, hepatitis B virus; HCV, hepatitis C virus.

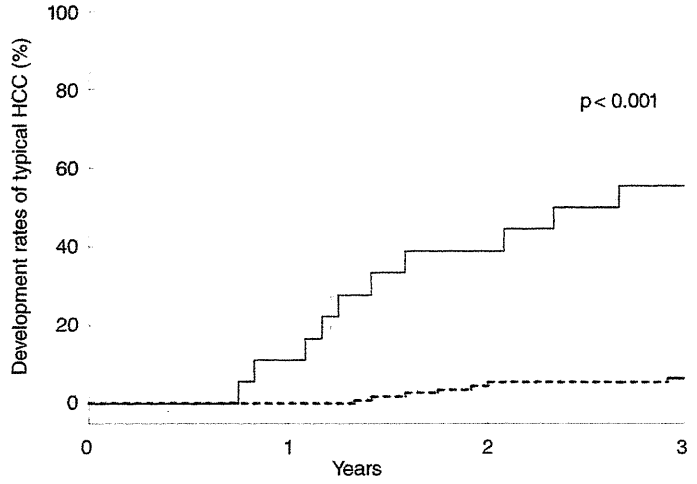

Figure 2 Cumulative incidence rates of typical hepatocellular carcinoma (HCC) development in the non-clean and clean liver groups. —, non-clean liver group ($n = 18$); ----, clean liver group ($n = 109$).

let count (HR, 1.17; 95% CI, 1.03–1.35; $P = 0.017$) and a non-clean liver (HR, 9.41; 95% CI, 3.47–25.46; $P < 0.001$) were the only independent risk factors for HCC development (Table 2).

We further assessed the effect of a non-clean liver on the risk of HCC development in subgroups of these patients (Fig. 4). We found that belonging to the non-clean liver group was a significant risk factor in patients without HBV. Notably, this designation was particularly valuable for patients who are generally regarded as at low risk for HCC development: those without cirrhosis (HR, 37.23; 95% CI, 3.30–419.71; $P = 0.003$) and those with high platelet counts (HR, 33.42; 95% CI, 6.69–166.94; $P < 0.001$).

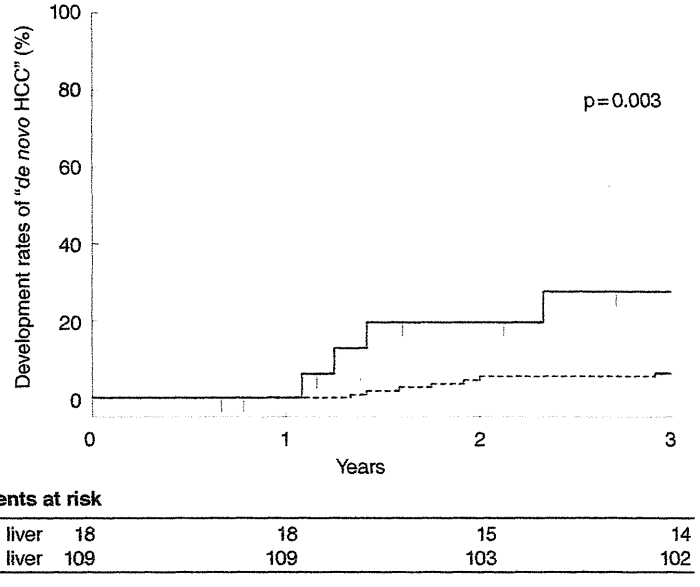

Figure 3 Cumulative incidence rates of typical hepatocellular carcinoma (HCC) at sites in which no nodules had been seen on the initial gadoxetic acid-enhanced magnetic resonance imaging, namely, "de novo HCC". —, non-clean liver group ($n = 18$); ----, clean liver group ($n = 109$).

Table 2 Variables that predict HCC development: univariate and multivariate analyses

Variables	Univariate		Multivariate	
	Hazard ratio (95% CI)	*P*	Hazard ratio (95% CI)	*P*
Male	0.56 (0.29–1.95)	0.755		
Age (per year)	1.06 (1.00–1.12)	0.039	1.08 (1.01–1.16)	0.024
Cirrhosis	14.37 (1.90–108.44)	0.009	3.54 (0.37–33.77)	0.231
HCV (vs HBV)	4.39 (0.58–33.17)	0.151		
Platelet count (per 10^{10}/L)	1.19 (1.06–1.33)	0.003	1.17 (1.03–1.35)	0.017
ALT (per IU/L)	1.00 (0.99–1.02)	0.423		
γ-GT (per IU/L)	1.00 (0.99–1.01)	0.688		
AFP >10 ng/mL	3.98 (1.47–10.77)	0.006	1.47 (0.49–4.33)	0.486
Non-clean liver	12.36 (4.68–32.61)	<0.001	9.41 (3.47–25.46)	<0.001

γ-GT, γ-glutamyltransferase; AFP, α-fetoprotein; ALT, alanine aminotransferase; CI, confidence interval; HBV, hepatitis B virus; HCC, hepatocellular carcinoma; HCV, hepatitis C virus.

DISCUSSION

THIS STUDY REVEALED presence of hypovascular hypointense liver nodules (non-clean liver) on gadoxetic acid-enhanced MRI, is a significant risk factor for subsequent development of typical HCC not only at the same sites but also at the different sites from the initial nodules. The incidence of development of typical HCC in the non-clean liver patients was more than 50% during a 3-year follow-up period, indicating that these higher risk patients should be rigorously investigated for the early detection of HCC during follow up.

In the present study, six of the 18 patients in the non-clean liver group developed typical HCC at the same site of the initial nodules during the subsequent 3 years (11.1%/year). Most of the hypovascular hypointense nodules on gadoxetic acid-enhanced MRI are considered precursor lesions of typical HCC, such as early HCC or high-grade dysplastic nodules, on histological examination,[13–15] while it has been reported that most hypovascular nodules exhibiting high-intensity to isointensity signals in the hepatocyte phase are benign hepatic nodules.[14,15] Recent studies have suggested that a reduction of organic anion-transporting polypeptide 1B3 (OATP 8) transporter expression begins at the earliest stage of hepatocarcinogenesis,[21,22] before changes in vascularity such as decreased portal flow or increased arterial flow. The progression rate of the small

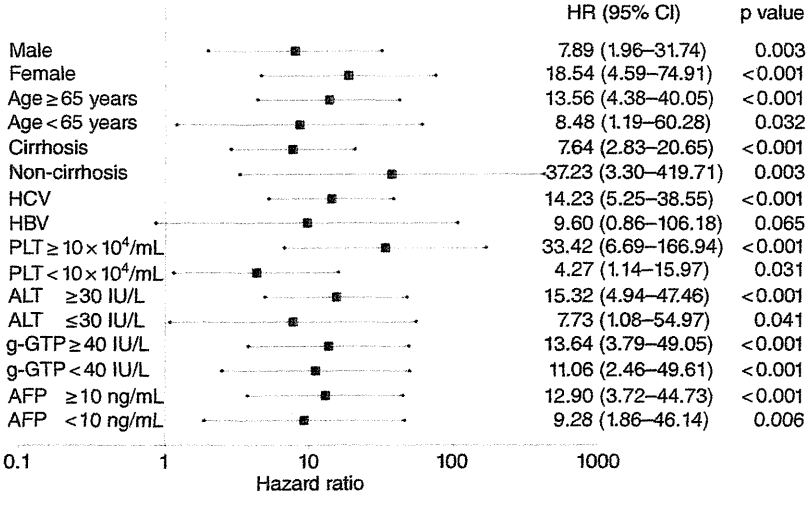

Figure 4 Stratified analyses of the non-clean liver as a risk factor for typical HCC development. AFP, α-fetoprotein; ALT, alanine aminotransferase; CI, confidence interval; g-GTP, γ-glutamyltransferase; HBV, hepatitis B virus; HCC, hepatocellular carcinoma; HCV, hepatitis C virus; HR, hazard ratio; PLT, platelets.

hypovascular hypointense nodules to typical HCC was reported as 10–17%/year,[9,10] which is comparable to the present study. Typical HCC arose exclusively among the nodules of 8 mm or more, as in previous studies in which the larger hypovascular hypointense nodules were found to be the risk factor for progression to typical HCC in the initial MRI study.[9,10]

Hyperintensity on T2WI[12] or diffusion-weighted images (DWI)[11] also was reported to be useful for prediction of typical HCC progress in hypovascular hypointense nodules. In our patients, none of the nodules in the non-clean liver group showed hyperintensity on T2WI, suggesting that the hepatocyte phase is more sensitive for detecting the early stage of hepatocarcinogenesis.[15] DWI were not evaluated in this study because this usually detects pathologically advanced HCC of larger size or with hypervascularity.[23] Thus, it is reasonable that the hepatocyte phase can effectively recognize the earliest stage of HCC development without T2WI or DWI.

In 11 of 17 patients, typical HCC developed at sites other than the initially detected hypovascular hypointense nodules. As shown in Figure 3, the incidence rates of such HCC in the non-clean liver group was significantly higher than in the clean liver group ($P = 0.003$), indicating that a non-clean liver itself is a risk factor for HCC development, apart from the detectable hypovascular hypointense nodules. In addition, in four patients with nodules even below 8 mm, two developed HCC at different sites from the initial nodules during follow up (data not shown). Taken together, a non-clean liver has the higher potential for hepatocarcinogenesis or for undetectable precursor lesions. The non-clean liver may reflect more advanced genetic or epigenetic changes in the background hepatocytes, however, the detailed biological mechanism is not clear in this study.

Non-clean liver was an independent risk factor for the development of typical HCC, apart from well-documented risk factors (Table 2), such as cirrhosis,[24] ALT,[25] γ-GT,[26] age and AFP.[27] A non-clean liver is a significant risk for HCC development also for those without cirrhosis or with high platelet counts (Fig. 4). This means patients at increased risk of HCC development can be discerned as having a non-clean liver even among low-risk subgroups.

Conversely, patients without such nodules (clean liver group) showed a significantly lower risk of developing typical HCC than those with non-clean livers (0.0% vs 11.1% at 1 year, 6.8% vs 55.5% at 3 years of follow up; $P < 0.001$), suggesting that gadoxetic acid-enhanced MRI could detect precursor lesions sensitively enough to rule out immediate (within 1 year) development of typical HCC. Although seven patients in the clean liver group developed typical HCC only after 1 year, these patients had other risk factors for HCC development, including lower platelet counts, implying more advanced liver cirrhosis or high AFP (data not shown). Such HCC may arise from precursor lesions that cannot be visualized by current imaging techniques.

This study is a retrospective study and has some limitations. We included patients with HBV and HCV together, because gadoxetic acid-enhanced MRI findings or HCC development do not differ between these two groups and HBV or HCV infection is not an independent risk factor for typical HCC development. However, the number of HBV patients was too small ($n = 26$) to statistically confirm the current result when limited to HBV patients only. Prospective studies with larger numbers of patients who have uniform liver disease etiologies and imaging intervals are needed to verify our findings in different settings. Although the imaging interval of the non-clean liver group was shorter than the clean liver group (3 vs 4 months: $P = 0.015$), the median intervals between the initial MRI and HCC diagnosis was 16 months in the non-clean liver group and 21 months in the clean liver group. They are short enough for cumulative detection of HCC development for 3 years and it is assumed that there was little influence on the conclusions.

In conclusion, patients with chronic viral liver disease are at high risk for developing typical HCC at any sites of the liver if they have hypovascular hypointense nodules on gadoxetic acid-enhanced MRI. These patients should be closely followed up for developing typical HCC not only at the same site but also at different sites from the initial nodule.

REFERENCES

1 Ichikawa T, Saito K, Yoshioka N *et al.* Detection and characterization of focal liver lesions: a Japanese phase III, multicenter comparison between gadoxetic acid disodium-enhanced magnetic resonance imaging and contrast-enhanced computed tomography predominantly in patients with hepatocellular carcinoma and chronic liver disease. *Invest Radiol* 2010; **45**: 133–41.
2 Halavaara J, Breuer J, Ayuso C *et al.* Liver tumor characterization: comparison between liver-specific gadoxetic acid disodium-enhanced MRI and biphasic CT – a multicenter trial. *J Comput Assist Tomogr* 2006; **30**: 345–54.
3 Hamm B, Staks T, Muhler A *et al.* Phase I clinical evaluation of Gd-EOB-DTPA as a hepatobiliary MR contrast

agent: safety, pharmacokinetics, and MR imaging. *Radiology* 1995; **195**: 785–92.
4 Hammerstingl R, Huppertz A, Breuer J *et al.* European EOB-study group. Diagnostic efficacy of gadoxetic acid (Primovist)-enhanced MRI and spiral CT for a therapeutic strategy: comparison with intraoperative and histopathologic findings in focal liver lesions. *Eur Radiol* 2008; **18**: 457–67.
5 Huppertz A, Balzer T, Blakeborough A *et al.* European EOB Study Group. Improved detection of focal liver lesions at MR imaging: multicenter comparison of gadoxetic acid-enhanced MR images with intraoperative findings. *Radiology* 2004; **230** (1): 266–75.
6 Di Martino M, Marin D, Guerrisi A *et al.* Intraindividual comparison of gadoxetate disodium-enhanced MR imaging and 64-section multidetector CT in the detection of hepatocellular carcinoma in patients with cirrhosis. *Radiology* 2010; **256**: 806–16.
7 Inoue T, Kudo M, Komuta M *et al.* Assessment of Gd-EOB-DTPA-enhanced MRI for HCC and dysplastic nodules and comparison of detection sensitivity versus MDCT. *J Gastroenterol* 2012; **47**: 1036–47.
8 Golfieri R, Renzulli M, Lucidi V, Corcioni B, Trevisani F, Bolondi L. Contribution of the hepatobiliary phase of Gd-EOB-DTPA-enhanced MRI to dynamic MRI in the detection of hypovascular small (</= 2 cm) HCC in cirrhosis. *Eur Radiol* 2011; **21**: 1233–42.
9 Kumada T, Toyoda H, Tada T *et al.* Evolution of hypointense hepatocellular nodules observed only in the hepatobiliary phase of gadoxetate disodium-enhanced MRI. *AJR Am J Roentgenol* 2011; **197** (1): 58–63.
10 Motosugi U, Ichikawa T, Sano K *et al.* Outcome of hypovascular hepatic nodules revealing no gadoxetic acid uptake in patients with chronic liver disease. *J Magn Reson Imaging* 2011; **34** (1): 88–94.
11 Kim YK, Lee WJ, Park MJ, Kim SH, Rhim H, Choi D. Hypovascular hypointense nodules on hepatobiliary phase gadoxetic acid-enhanced MR images in patients with cirrhosis: potential of DW imaging in predicting progression to hypervascular HCC. *Radiology* 2012; **265** (1): 104–14.
12 Hyodo T, Murakami T, Imai Y *et al.* Hypovascular nodules in patients with chronic liver disease: risk factors for development of hypervascular hepatocellular carcinoma. *Radiology* 2013; **266**: 480–90.
13 Bartolozzi C, Battaglia V, Bargellini I *et al.* Contrast-enhanced magnetic resonance imaging of 102 nodules in cirrhosis: correlation with histological findings on explanted livers. *Abdom Imaging* 2013; **38**: 290–6.
14 Golfieri R, Grazioli L, Orlando E *et al.* Which is the best MRI marker of malignancy for atypical cirrhotic nodules: hypointensity in hepatobiliary phase alone or combined with other features? Classification after Gd-EOB-DTPA administration. *J Magn Reson Imaging* 2012; **36**: 648–57.
15 Sano K, Ichikawa T, Motosugi U *et al.* Imaging study of early hepatocellular carcinoma: usefulness of gadoxetic acid-enhanced MR imaging. *Radiology* 2011; **261**: 834–44.
16 Motosugi U. Hypovascular hypointense nodules on hepatocyte phase gadoxetic acid-enhanced MR images: too early or too progressed to determine hypervascularity. *Radiology* 2013; **267** (1): 317–8.
17 Asayama Y, Yoshimitsu K, Nishihara Y *et al.* Arterial blood supply of hepatocellular carcinoma and histologic grading: radiologic-pathologic correlation. *AJR Am J Roentgenol* 2008; **190** (1): W28–34.
18 Motosugi U, Ichikawa T, Sou H *et al.* Liver parenchymal enhancement of hepatocyte-phase images in Gd-EOB-DTPA-enhanced MR imaging: which biological markers of the liver function affect the enhancement? *J Magn Reson Imaging* 2009; **30**: 1042–6.
19 Bruix J, Sherman M, American Association for the Study of Liver Diseases. Management of hepatocellular carcinoma: an update. *Hepatology* 2011; **53**: 1020–2.
20 Motosugi U, Ichikawa T, Araki T. Rules, roles, and room for discussion in gadoxetic acid-enhanced magnetic resonance liver imaging: current knowledge and future challenges. *Magnetic Rsonance in Medical Sciences.* 2013; **12**: 161–75.
21 Kitao A, Zen Y, Matsui O *et al.* Hepatocellular carcinoma: signal intensity at gadoxetic acid-enhanced MR imaging – correlation with molecular transporters and histopathologic features. *Radiology* 2010; **256**: 817–26.
22 Narita M, Hatano E, Arizono S *et al.* Expression of OATP1B3 determines uptake of Gd-EOB-DTPA in hepatocellular carcinoma. *J Gastroenterol* 2009; **44**: 793–8.
23 Nasu K, Kuroki Y, Tsukamoto T, Nakajima H, Mori K, Minami M. Diffusion-weighted imaging of surgically resected hepatocellular carcinoma: imaging characteristics and relationship among signal intensity, apparent diffusion coefficient, and histopathologic grade. *American Journal of Roentgenology* 2009; **193**: 438–44.
24 Degos F, Christidis C, Ganne-Carrie N *et al.* Hepatitis C virus related cirrhosis: time to occurrence of hepatocellular carcinoma and death. *Gut* 2000; **47** (1): 131–6.
25 Tarao K, Rino Y, Ohkawa S *et al.* Association between high serum alanine aminotransferase levels and more rapid development and higher rates of incidence of hepatocellular carcinoma in patients with hepatitis C virus-associated cirrhosis. *Cancer* 1999; **86**: 589–95.
26 Ikeda K, Saitoh S, Suzuki Y *et al.* Disease progression and hepatocellular carcinogenesis in patients with chronic viral hepatitis: a prospective observation of 2215 patients. *J Hepatol* 1998; **28**: 930–8.
27 Ikeda K, Saitoh S, Koida I *et al.* A multivariate analysis of risk factors for hepatocellular carcinogenesis: a prospective observation of 795 patients with viral and alcoholic cirrhosis. *Hepatology* 1993; **18** (1): 47–53.

J Gastroenterol (2014) 49:163–164
DOI 10.1007/s00535-013-0926-7

EDITORIAL

Once-daily simeprevir in combination with pegylated-interferon and ribavirin: a new horizon in the era of direct-acting antiviral agent therapy for chronic hepatitis C

Shinya Maekawa · Nobuyuki Enomoto

Received: 7 December 2013 / Accepted: 10 December 2013 / Published online: 21 December 2013

Hepatitis C virus (HCV) is a leading cause of chronic hepatitis, liver cirrhosis, and hepatocellular carcinoma (HCC), and it is estimated that infected individuals total 185 million people worldwide. In Japan, around 2 million are infected with HCV, and more than 20 thousand die from HCV-induced HCC annually. Though viral eradication with antiviral therapies is the most important and effective choice for decreasing HCC-related deaths induced by HCV, complete viral eradication has been quite difficult till recently, especially in patients with genotype-1 HCV infection because of the low response rate to interferon (IFN)-based therapy [1, 2].

In this background, development of novel direct-acting antiviral agents (DAAs) specific for HCV was truly a revolutionary event. In 2011, two first-generation NS3 protease inhibitors (PIs), telaprevir and boceprevir, were firstly approved among all the DAAs for clinical use in USA and Europe for genotype-1 HCV in combination with pegylated-interferon and ribavirin (PR), while telaprevir was approved in Japan in the same 2011 period. As expected, a regimen including telaprevir in combination with pegylated-interferon and ribavirin dramatically improved the sustained viral response (SVR) rate to as high as 80 % in genotype-1 HCV infection. On the other hand, telaprevir has several undesirable problems. Among all, adverse events (AEs) of anemia and skin rash are serious problems of telaprevir, and Grade 3/4 skin disorders, including Stevens–Johnson syndrome and drug rashes with eosinophilia and systemic symptoms, as well as Grade 3 anemia (<8.0 g/dL), might occur [3, 4]. Moreover, cumbersome frequent dosing three times a day (every 7–9 h) could induce poor medication adherence. Under the circumstances, it has been quite stressful for patients as well as clinicians to introduce and monitor this telaprevir-based regimen.

Simeprevir (SMV, TMC435) is classified as a second-generation PI with the macrocyclic structure having an advantage in the binding affinity and specificity for NS3 protease compared to the first-generation PI with the linear structure. Due to the difference in the structure, the drug-resistance profile is somewhat different from that of telaprevir. Though simeprevir shows cross-resistance with telaprevir at amino acid positions of 155 and 156, most of the resistant mutation occurs at the simeprevir-specific amino acid position of 168 [5]. Though simeprevir is effective in all viral genotypes (genotype 1–6), it has the strongest antiviral activity for genotype-1a and -1b HCV infection. In particular, low AE rate and its patient-friendly once-daily dosing are the important characters of simeprevir aside from its strong antiviral activity. In the international phase II trials of simeprevir in combination with PegIFNa-2a/RBV for treatment-naïve (PILLAR study) [6] and treatment-experienced patients (ASPIRE study) [7] for HCV genotype 1-infected patients, it was demonstrated that simeprevir was generally well tolerated and had a pharmacokinetic profile supporting once-a-day (QD) dosing resulting in high virologic response rates.

In this issue of the *Journal of Gastroenterology*, Hayashi et al. [8] reported the important results of the phase II *D*ose and duration *R*anging study of *A*ntiviral agent TMC435 in *G*enotype *O*ne HCV treatment-*N*aïve patients (DRAGON study; TMC435-C215) evaluating once-daily simeprevir

This comment refers to the article available at doi:10.1007/s00535-013-0875-1.

S. Maekawa (✉) · N. Enomoto
First Department of Internal Medicine, Faculty of Medicine, University of Yamanashi, 1110 Shimokato, Chuo, Yamanashi 409-3898, Japan
e-mail: maekawa@yamanashi.ac.jp

with pegylated-interferon and ribavirin therapy for treatment-naïve, high viral-loaded hepatitis C genotype 1-infected patients in Japan. Due to the result of previous phase I study that simeprevir plasma concentration was higher in Japanese healthy volunteers compared with Caucasian volunteers, simeprevir doses of 50/100 mg QD were selected for this study, while simeprevir doses of 150 mg QD were selected in western countries [9]. Through investigating five treatment groups (SMV12/PR24 50 mg, SMV12/PR24 100 mg, SMV24/PR24 50 mg, SMV24/PR24 100 mg, and PR48), it was disclosed that simeprevir-combined groups all achieved high SVR rate (77–92 % compared to 46 % for PR). As to the AEs, simeprevir was well tolerated, and the incidence of anemia and skin rash were similar in their frequency and their grade between all the SMV groups and the PR group. Due to low AEs, therapy discontinuation rate and ribavirin dose reduction was also similar in the SMV groups and the PR group. While an AE of bilirubin elevation was specific to simeprevir, and it reached to grade 3 (2.6–5.0 mg/dL) to 4 (>5.0 mg/dL) in four patients (5 %) leading to the discontinuation of simeprevir in these individuals, the bilirubin level returned to baseline after the end of simeprevir in those patients. Since bilirubin elevation is considered to result from the blockade of bilirubin clearance-associated OATP1B1 and MRP transporters by simeprevir [10], it is considered that the bilirubin elevation by simeprevir does not reflect deterioration of liver function.

Following the results of this phase II DRAGON study, treatment dosage of simeprevir was determined as 100 mg QD in Japan, and successive phase III CONCERTO studies for simeprevir/pegylated-interferon/ribavirin therapy have been conducted (CONCERTO-1 for treatment-naïve, -2 for previous null responder, -3 for previous relapser, and -4 for naïve, null responder and relapser). After the completion of those CONCERTO studies with favorable outcomes for simeprevir-based regimens, once-daily simeprevir with pegylated-interferon and ribavirin therapy for high viral-loaded hepatitis C genotype 1-infected patients was just recently approved for clinical use in Japan.

Considering the history of HCV therapy, this new therapy of once-daily simeprevir with pegylated-interferon and ribavirin therapy is ideal in its high efficacy and low AEs. Of course, it is true that DAA combination therapies without IFN (IFN-free therapies) would appear in the near future, and that these IFN-free therapies are advantageous in that they are free from IFN-related AEs. However, in terms of DAA-resistant viral mutants, it is considered that these mutant HCVs generally have low replication fitness, and are sensitive to IFN. Therefore, it is speculated that IFN-based DAA therapies compared to IFN-free DAA therapies are safer in preventing the development of multidrug resistant HCVs.

Taken together, the new regimen of once-daily simeprevir with pegylated-interferon and ribavirin therapy would surely be an important milestone in the therapy for high viral-loaded hepatitis C genotype-1 infected patients in the era of DAA therapy.

References

1. Kim MN, Kim BK, Han KH. Hepatocellular carcinoma in patients with chronic hepatitis C virus infection in the Asia-Pacific region. J Gastroenterol. 2013;48(6):681–8.
2. Thomas DL. Global control of hepatitis C: where challenge meets opportunity. Nat Med. 2013;19(7):850–8.
3. Chayama K, Hayes CN, Ohishi W, Kawakami Y. Treatment of chronic hepatitis C virus infection in Japan: update on therapy and guidelines. J Gastroenterol. 2013;48(1):1–12.
4. Kumada H, Toyota J, Okanoue T, Chayama K, Tsubouchi H, Hayashi N. Telaprevir with peginterferon and ribavirin for treatment-naive patients chronically infected with HCV of genotype 1 in Japan. J Hepatol. 2013;56(1):78–84.
5. Lenz O, Verbinnen T, Lin TI, Vijgen L, Cummings MD, Lindberg J, et al. In vitro resistance profile of the hepatitis C virus NS3/4A protease inhibitor TMC435. Antimicrob Agents Chemother. 2010;54(5):1878–87.
6. Fried MW, Buti M, Dore GJ, Flisiak R, Ferenci P, Jacobson I, et al. Once-daily simeprevir (TMC435) with pegylated interferon and ribavirin in treatment-naive genotype 1 hepatitis C: the randomized PILLAR study. Hepatology. 2013;58(6):1918–29.
7. Zeuzem S, Berg T, Gane E, Ferenci P, Foster GR, Fried MW, et al. Simeprevir increases rate of sustained virologic response among treatment-experienced patients with HCV genotype-1 infection: a phase IIb trial. Gastroenterology. 2013. doi:10.1053/j.gastro.2013.10.058.
8. Hayashi N, Seto C, Kato M, Komada Y, Goto S. Once-daily simeprevir (TMC435) with peginterferon/ribavirin for treatment-naïve hepatitis C genotype 1-infected patients in Japan: the DRAGON study. J Gastroenterol. 2013. doi:10.1007/s00535-013-0875-1.
9. Verloes R, Shishido A. Phase I safety and PK of TMC435 in healthy volunteers and safety, PK and short-term efficacy in chronic hepatitis C infected individuals. Kobe: Abstract O-32 presented at the Japanese Hepatology Congress; 2009. p. 4–5.
10. Huisman MT, Snoeys J, Monbaliu J, Martens M, Sekar V, Raoof A. In vitro studies investigating the mechanism of interaction between TMC435 and hepatic transporters. Poster 278 presented at the 61st Annual Meeting of the American Association for the Study of Liver Diseases (AASLD), Boston, USA, October 29–November 2, 2010.

JVI
Journals.ASM.org

Deep-Sequencing Analysis of the Association between the Quasispecies Nature of the Hepatitis C Virus Core Region and Disease Progression

Mika Miura,[a] Shinya Maekawa,[a] Shinichi Takano,[a] Nobutoshi Komatsu,[a] Akihisa Tatsumi,[a] Yukiko Asakawa,[a] Kuniaki Shindo,[a] Fumitake Amemiya,[a] Yasuhiro Nakayama,[a] Taisuke Inoue,[a] Minoru Sakamoto,[a] Atsuya Yamashita,[b] Kohji Moriishi,[b] Nobuyuki Enomoto[a]

First Department of Internal Medicine, Faculty of Medicine, University of Yamanashi, Shimokato, Chuo, Yamanashi, Japan[a]; Department of Microbiology, University of Yamanashi, Shimokato, Chuo, Yamanashi, Japan[b]

Variation of core amino acid (aa) 70 of hepatitis C virus (HCV) has been shown recently to be closely correlated with liver disease progression, suggesting that the core region might be present as a quasispecies during persistent infection and that this quasispecies nature might have an influence on the progression of disease. In our investigation, the subjects were 79 patients infected with HCV genotype 1b (25 with chronic hepatitis [CH], 29 with liver cirrhosis [LC], and 25 with hepatocellular carcinoma [HCC]). Deep sequencing of the HCV core region was carried out on their sera by using a Roche 454 GS Junior pyrosequencer. Based on a plasmid containing a cloned HCV sequence (pCV-J4L6S), the background error rate associated with pyrosequencing, including the PCR procedure, was calculated as 0.092 ± 0.005/base. Deep sequencing of the core region in the clinical samples showed a mixture of "mutant-type" Q/H and "wild-type" R at the core aa 70 position in most cases (71/79 [89.9%]), and the ratio of mutant residues to R in the mixture increased as liver disease advanced to LC and HCC. Meanwhile, phylogenetic analysis of the almost-complete core region revealed that the HCV isolates differed genetically depending on the mutation status at core aa 70. We conclude that the core aa 70 mixture ratio, determined by deep sequencing, reflected the status of liver disease, demonstrating a significant association between core aa 70 and disease progression in CH patients infected with HCV genotype 1b.

Hepatitis C virus (HCV)-related liver disease gradually advances from chronic hepatitis (CH) to liver cirrhosis (LC) and to hepatocellular carcinoma (HCC) over 20 to 30 years (1). However, the rates of disease progression differ: some patients develop HCC over several years, while others show persistently normal alanine aminotransferase (PNALT) levels for decades, and the cause of the difference remains poorly understood.

The involvement of viral and host factors in the progression of liver disease and hepatocarcinogenesis is complex (2). With regard to viral factors, the relationship between the viral core region and disease progression in HCV genotype 1b infection has attracted clinical attention. Specifically, it has been reported that the core amino acid (aa) 70 residue, identified as a variable related to the outcome of interferon (IFN) therapy (3), is closely associated with the progression of hepatitis and hepatocarcinogenesis in Japan and North America (4–7). Those previous studies and our own have reported that core aa 70 variation is strongly linked to carcinogenesis and that substitutions in the core aa 70 region aggravate hepatitis and heighten the risk of hepatocarcinogenesis during the clinical course, corroborating the relationship between the status of the core region and disease progression (8, 9).

With regard to host factors, a genomewide association study (GWAS) has recently shown that single nucleotide polymorphisms (SNPs) around the interleukin 28B (IL28B) gene (rs12979860 and rs8099917), encoding the type III IFN IFN-λ3, are strongly correlated with the outcomes of therapy with pegylated IFN-α plus ribavirin for chronic hepatitis C (CH-C) (10–13). Interestingly, in contrast to the core region, consensus has not been reached as to the relationship between disease progression and the IL28B SNP, which is associated with IFN resistance (14–17). Previously, we reported that there was no correlation between the onset of HCC and the IL28B SNP (9). However, it was reported that the IL28B rs8099917 TG/GG allele was markedly correlated with the presence of Q (glutamine) or H (histidine) instead of the R (arginine) residue at core aa 70, while the IL28B rs8099917 TT allele was correlated with core aa 70R (8). Moreover, the core amino acid R70Q/H change occurs more often in patients with IL28B rs8099917 TG/GG than in those with IL28B rs8099917 TT (9). In this manner, the contributions of the core aa 70 residue and the IL28B SNP, which were found to be IFN sensitivity factors, to the progression of liver disease have gradually been elucidated.

HCV exists in a host as a swarm of variants, known as a "quasispecies," and this quasispecies nature has been considered to play a critical role in pathogenesis (18). However, detailed analysis has been technically difficult, and the clinical significance has not been clarified in detail thus far. Considering the observation of core aa 70 gene changes over time, it is assumed that a variety of core aa 70 isolates may exist as a quasispecies, and this could be related to pathogenesis as described above.

Recently, deep-sequencing technology has advanced rapidly and has enabled us to analyze viral quasispecies in association with the status of the disease (19–22). In this study, we investigated how the quasispecies of the HCV core gene, either at the hot spot of the core aa 70 residue or in the almost-entire core gene, is created and is involved in disease progression in patients with CH-C.

Received 28 March 2013 Accepted 7 August 2013
Published ahead of print 14 August 2013
Address correspondence to Shinya Maekawa, maekawa@yamanashi.ac.jp.
Supplemental material for this article may be found at http://dx.doi.org/10.1128/JVI.00826-13.

doi:10.1128/JVI.00826-13

TABLE 1 Patient characteristics classified by disease progression

Characteristic[a]	Value for patients with:			P
	CH (n = 25)	LC (n = 29)	HCC (n = 25)	
No. male/female	14/11	10/19	12/13	0.278
Age (yr) (mean ± SD)	63.4 ± 14.6	66.5 ± 9.2	68.4 ± 8.2	0.539
Platelets (10^{-4}/mm^3) (mean ± SD)	16.1 ± 4.7	9.8 ± 3.9	11.1 ± 5.1	<0.001
Albumin (g/dl) (mean ± SD)	4.4 ± 0.3	3.9 ± 0.6	3.5 ± 0.5	<0.001
γ-GTP (IU/liter) (median [range])	53.5 (12–230)	38.0 (12–108)	40.8 (15–110)	0.845
T. chol. (mg/dl) (mean ± SD)	161 ± 28	148 ± 30	140 ± 28	0.053
HCV RNA (kIU/ml) (median [range])	7,047 (501–19,953)	5,369 (126–25,119)	8,421 (110–25,119)	0.288
Alpha-fetoprotein (ng/ml) (median [range])	5.0 (1.1–16.5)	32.2 (1.0–252.6)	614.8 (1.9–13,418)	<0.001
AST (IU/liter) (mean ± SD)	42.4 ± 17.8	51.1 ± 23.5	59.1 ± 28.2	0.046
ALT (IU/liter) (mean ± SD)	46.6 ± 23.1	43.9 ± 29.3	60.7 ± 52.7	0.263
No. with R/(Q/H) at core aa 70[b]	19/6	12/17	8/17	0.005
No. with L/(M/C) at core aa 91[b]	17/8	19/10	15/10	0.834
No. of ISDR mutations (median [range])[b]	0.8 (0–6)	1.2 (0–7)	0.9 (0–8)	0.799
No. of IRRDR mutations (median [range])[b]	4.9 (1–10)	4.7 (2–9)	5.2 (1–12)	0.962
No. with TT/non-TT at IL28B SNP (rs8099917)	18/7	17/12	14/11	0.458
No. without/with a history of interferon therapy	14/11	16/13	15/10	0.933

[a] T. chol., total cholesterol; AST, aspartate transaminase; ALT, alanine aminotransferase.
[b] Core aa 70, core aa 91, the interferon sensitivity-determining region (ISDR), and the interferon-ribavirin resistance-determining region (IRRDR) were dominant viral sequences determined by direct sequencing.

PATIENTS AND METHODS

Patients. The subjects were 79 patients persistently infected with HCV genotype 1b who were followed up at Yamanashi University Hospital. The patients all fulfilled the following criteria: (i) they were negative for hepatitis B surface antigen; (ii) they had no other forms of hepatitis, such as primary biliary cirrhosis, autoimmune liver disease, or alcoholic liver disease; (iii) they were free of coinfection with human immunodeficiency virus; and (iv) signed consent was obtained for the study protocol. The study protocol had been approved by the Human Ethics Review Committee of Yamanashi University Hospital and conformed to the ethical guidelines of the Declaration of Helsinki.

The breakdown was as follows: 25 patients with CH, 29 with LC, and 25 with HCC. The patients' clinical backgrounds, including histories of interferon-based antiviral therapy, are shown in Table 1. Deep-sequencing analysis was performed using serum samples taken at the most recent visit from patients with chronic hepatitis or liver cirrhosis and at the first diagnosis of HCC from patients with HCC. A direct-sequencing method, which determines the dominant viral sequence, was performed as described previously (9) to determine the dominant viral sequences of the core region, the interferon sensitivity-determining region (ISDR), and the interferon-ribavirin resistance-determining region (IRRDR) from the serum of each patient.

Deep sequencing. Deep sequencing of the viral core region was performed for each of 79 patients. Briefly, RNA was extracted from the stored sera of these patients and was reverse transcribed to cDNA. Then two-step nested PCR was carried out with primers specific for the core region of the HCV genome (23). The primers for the second-round PCR had barcodes attached, were 10 nucleotides (nt) long, and differed for each sample, so that PCR products from each sample were identifiable (see Table S1 in the supplemental material). After the band densities of the PCR products were quantified using a Bioanalyzer (Agilent Technologies, Palo Alto, CA), the concentrations of the samples were adjusted to a common value, and pooled samples were prepared. Libraries were then subjected to emulsion PCR, the enriched DNA beads loaded onto a picotiter plate, and pyrosequencing carried out with a Roche GS Junior/454 sequencing system using titanium chemistry (Roche, Branford, CT). In order to determine the error rate of the procedure, deep sequencing was carried out under similar conditions with a plasmid containing a cloned HCV sequence (pCV-J4L6S) (24). Amplicon Variant Analyzer software, version 2.5p1 (Roche), was used for analysis.

A dominant sequence of the core region for each patient was deposited in GenBank. Although the study amplified 499 nucleotides, from the 25th to the 523rd nucleotide of the core region, by PCR (Fig. 1), information for only 459 of the 499 nucleotides was uploaded for each patient, since some minor PCR amplicons obtained by deep sequencing did not include the full 499 nucleotides.

Phylogenetic tree analysis. Phylogenetic trees were constructed from the sequences by using the neighbor-joining method with BioEdit and MEGA5.05, and bootstrapping was performed with 1,000 replicates (25). In constructing phylogenetic trees, the three bases of the core codon 70 were removed in the analysis of all trees, since the mutation rate of other parts of the core region is known to be rather low, and it was possible that the influence of the core aa 70 mutations might be overestimated in the phylogenetic trees. In addition, using genetic distance data obtained from the phylogenetic analysis, the genetic distances between every two HCVs with core aa 70R, between every two HCVs with a residue other than R at core aa 70 (core aa 70non-R), and between every two HCVs with different residues at core aa 70 (one HCV with R and one with a non-R residue) were also compared statistically in order to reveal the genetic associations among those HCV core subgroups.

Statistical analysis. Statistical differences in the parameters, including all available patients' demographic, biochemical, hematological, virological, and SNP data in the three groups (CH, LC, and HCC), were determined using the Kruskal-Wallis test. The Mann-Whitney U test was used for statistical differences in numerical variables between two groups. Trends for categorical data

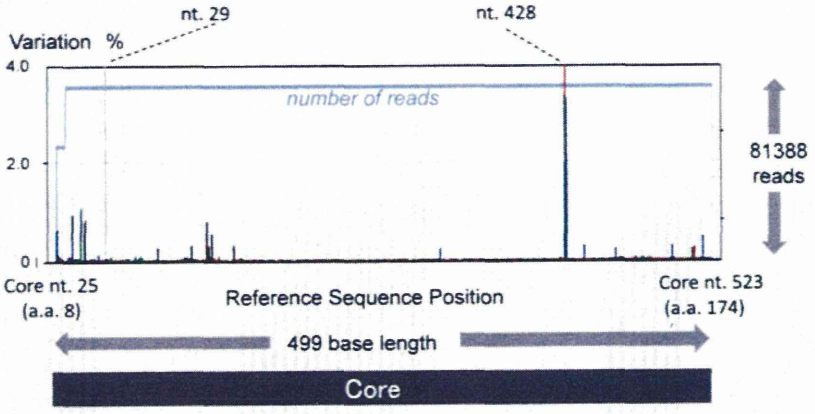

FIG 1 The core region of pCV-J4L6S (genotype 1b) from the 25th to the 523rd nucleotide, and from the 9th to the 174th codon, was subjected to deep sequencing, and the background error rate of pyrosequencing was calculated. In order to show rare background errors, those errors with low percentages are magnified.

were evaluated using the Cochran-Armitage trend test. All *P* values of <0.05 by the two-tailed test were considered significant in comparisons of genetic distances.

Nucleotide sequence accession numbers. The dominant sequences of the core regions from the patient samples have been deposited in GenBank under accession numbers AB822372.1 to AB822459.1.

RESULTS

Calculation of background errors in deep sequencing. First, the background error rate of pyrosequencing was calculated with a plasmid containing a cloned HCV sequence (pCV-J4L6S). Figure 1 shows the results of deep sequencing from the 25th to the 523rd nucleotide of the core region (499 nt) in pCV-J4L6S. Among 81,388 reads, each 499 nt long, the maximum error rate was 99.14% at the 428th base, and the next highest error rate was 64.17% at the 29th base. A six-C homopolymer region ending at the 428th base was read as a five-C homopolymer and a five-A homopolymer region ending at the 29th base was read as a four-A homopolymer in most of the obtained sequences; these homopolymer sequences are a weak point of pyrosequencing (26, 27).

A base appearing six times consecutively was the longest sequence of identical repeated nucleotides and was found only at the 428th nt position in the core region of pCV-J4L6S. Five consecutive bases were found at two sites (the 336th and 436th nt) in addition to the 29th nt position, but this error (i.e., the miscounting of homopolymer length) occurred only at the 29th base closest to the end of the sequence. Excluding the 428th and 29th nt positions, the error rate was ~1% or lower, as shown in Fig. 1. There was no single nucleotide error in the codons for aa 70 and aa 91in the repeated control experiments. From repeated deep sequencing of the plasmid, the overall nucleotide error rate was calculated as 0.092 ± 0.005 (mean ± standard deviation [SD])/base. Based on this analysis, a mixture of bases detectable above the background error of 0.102% (mean background error rate + 2 SDs) was defined as a real mixture.

Baseline characteristics. The baseline characteristics of the 79 patients are shown in Table 1. The values for viral factors core aa 70 and aa 91, NS5A-ISDR, and NS5A-IRRDR are the results of the direct-sequencing study. As shown in Table 1, the results for the variables platelets, albumin, alpha-fetoprotein, and core aa 70 differed significantly according to disease progression. On the other hand, no difference was observed in core aa 91 and IL28B SNP (rs8099917) according to disease progression.

Quasispecies nature of core amino acid 70 and disease progression. Deep sequencing of the core region was carried out with a variety of clinical samples. Simultaneous analysis was carried out using the barcoded primers, and approximately 950 reads were obtained per sample (Table 2). When the analysis was focused on core aa 70, the proportion of non-R (Q/H) sequences increased as disease severity advanced from CH to LC to HCC, as shown in Fig. 2A and Table 3 ($P = 0.018$). When a mixture of 0.102% or more was defined as a real mixture, deep sequencing showed the presence of a mixture at core aa 70 in 71 of the 79 patients (89.9%).

The relationship between disease progression and the occurrence of a quasispecies was also analyzed at the codon for core aa 91, which has also been reported to be associated with the outcomes of IFN therapy and the occurrence of HCC. As with core aa 70, a quasispecies was recognized at this site, and mixtures were observed in most patients. However, in contrast to the core aa 70 codon, there was no clear relationship with disease progression (Fig. 2B and Table 3).

Figure 2C and D show the correlation between mixtures in the core aa 70 and 91 regions and IL28B SNPs. As shown in Fig. 2C and Table 4, the proportion of mutations in the core aa 70 codon was highly dependent on the IL28B SNP (*P*, <0.005 [Table 4]). Such a relationship was also found between the proportion of mutations in core aa 91 and IL28B SNPs (Fig. 2D and Table 4), although its significance was rather weaker (*P*, 0.010).

TABLE 2 Amplicon read numbers obtained by deep sequencing of samples from 79 patients

Group	No. of patients	Total no. of reads	Avg no. of reads ± SD (range)/sample
CH	25	22,365	894.6 ± 222.8 (367–1,486)
LC	29	28,537	982.5 ± 258.1 (660–1,528)
HCC	25	24,284	971.4 ± 242.5 (405–1,749)
Total	79	75,186	951.7 ± 240.9 (367–1,749)

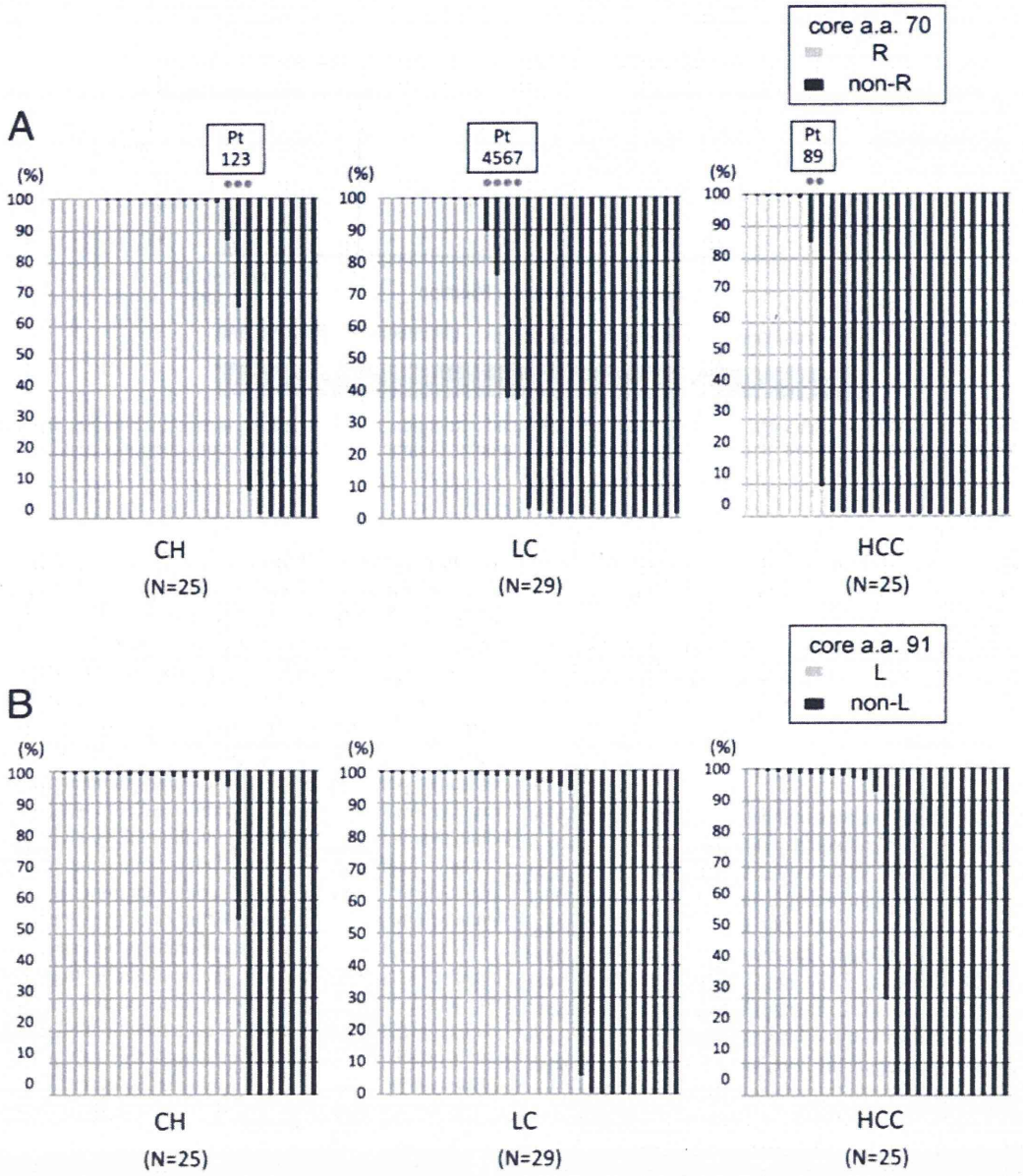

FIG 2 The core regions of the HCV genomes from 79 patients persistently infected with HCV genotype 1b (25 patients with chronic hepatitis [CH], 29 with liver cirrhosis [LC], and 25 with hepatocellular carcinoma [HCC]) were subjected to deep sequencing. Each bar represents the result for a single patient. At the specific locations of core aa 70 and aa 91, no single nucleotide mutation was observed in the previous control plasmid experiment. (A) Disease stages and percentages of mutations at core aa 70. Nine dots indicate the nine patients with a high mixture rate (between 5% and 95%) at core aa 70 (R and non-R). (B) Disease stages and percentages of mutations at core aa 91. (C) IL28B SNP and percentages of mutations at core aa 70. (D) IL28B SNP and percentages of mutations at core aa 91.

Since direct sequencing has also shown an association of several sites other than core aa 70 and 91 with the occurrence of HCC (6), those sites were also investigated for such an association. However, there was no clear relationship between these sites and disease progression, except for G209A (core aa R70Q) (see Fig. S1 and Table S2 in the supplemental material).

Phylogenetic tree analysis of HCV core region focusing on the core aa 70 residue. Because it was clear that the core aa 70 quasispecies state was significantly associated with disease progression, our next interest was to determine how this single hot spot is correlated with the remainder of the (almost-entire) core region. Therefore, phylogenetic tree analysis was performed, and genetic distances among aa 70-associated core sequences were also compared statistically. In constructing all phylogenetic trees, the three bases of the core 70 codon were removed, since the mutation rate of other parts of the core region is known to be rather low, and it was possible that the influence of the core aa 70 mutations might be overestimated in the phylogenetic trees.

At first, to determine the associations among the remainder of the core sequences across different patients, a phylogenetic tree was constructed for all 79 patients using dominant core sequences obtained from each patient. In constructing the tree, two domi-

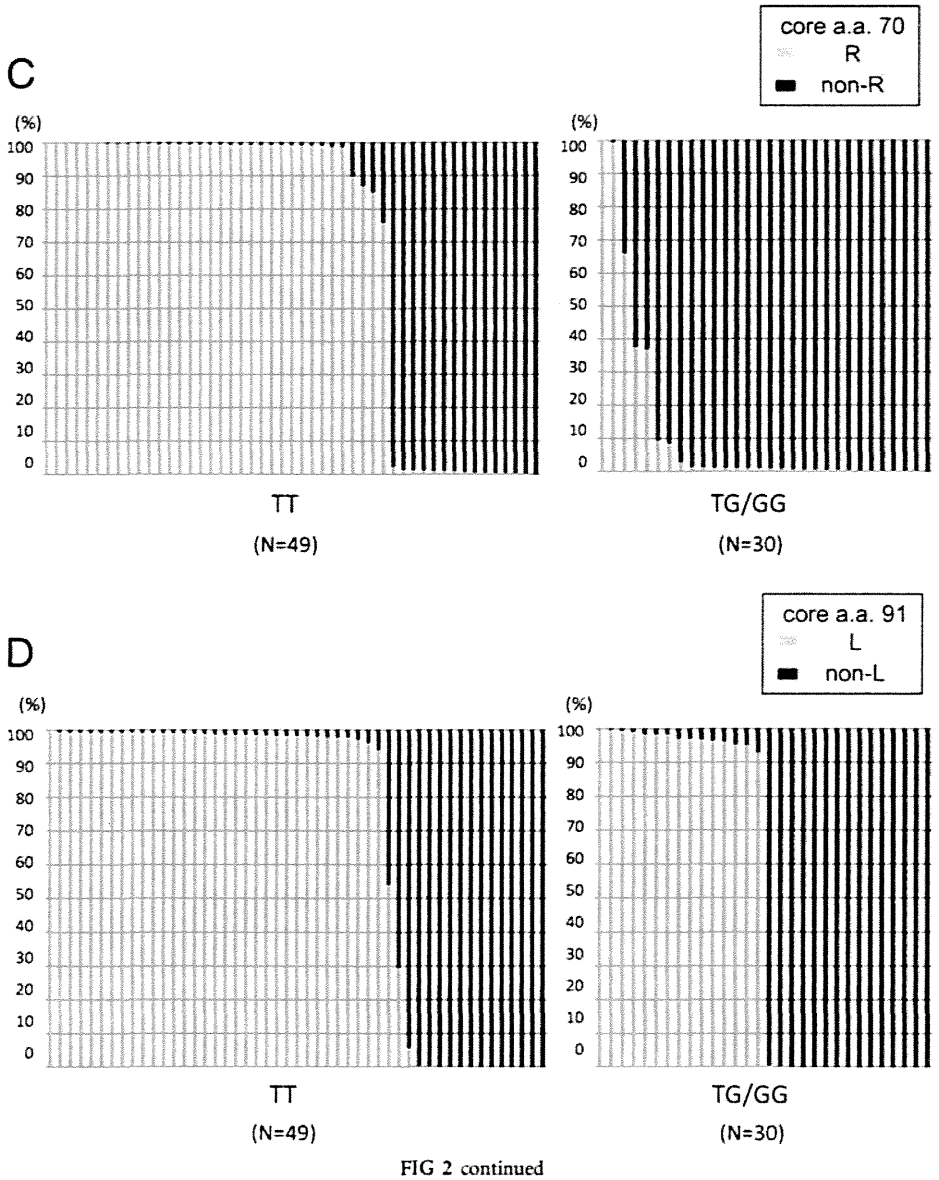

FIG 2 continued

nant sequences (the dominant core sequence in isolates with aa 70R and the dominant core sequence in isolates with aa 70non-R) were included in the analysis for each of the nine patients with high mixture rates (5% or more) of R and non-R at core aa 70 (Fig. 2A), while one dominant sequence each was included for other patients. As shown in Fig. 3A and Table 5, genetic distances calculated between every two core sequences with aa 70R (R-R) were significantly larger than those between two core sequences with aa 70non-R (non-R–non-R) or those between a

TABLE 3 Correlation between quasispecies composition and disease progression

Patient group (*n*)	Median % (range) with:	
	R at core aa 70[a]	L at core aa 91[b]
CH (25)	70.35 (0.00–100.00)	69.12 (0.00–99.40)
LC (29)	43.22 (0.24–100.00)	64.54 (0.00–99.50)
HCC (25)	28.20 (0.00–99.80)	52.23 (0.00–100.00)

[a] *P*, 0.018.
[b] *P*, 0.630.

TABLE 4 Correlation between quasispecies composition and IL28B SNP rs8099917

Group (sequence at IL28B SNP rs8099917)	Median % (range) with:	
	R at core aa 70[a]	L at core aa 91[b]
TT (*n* = 49)	68.15 (0.00–100.00)	68.24 (0.00–100.00)
TG/GG (*n* = 30)	12.64 (0.00–100.00)	48.76 (0.00–100.00)

[a] *P*, <0.005.
[b] *P*, 0.010.

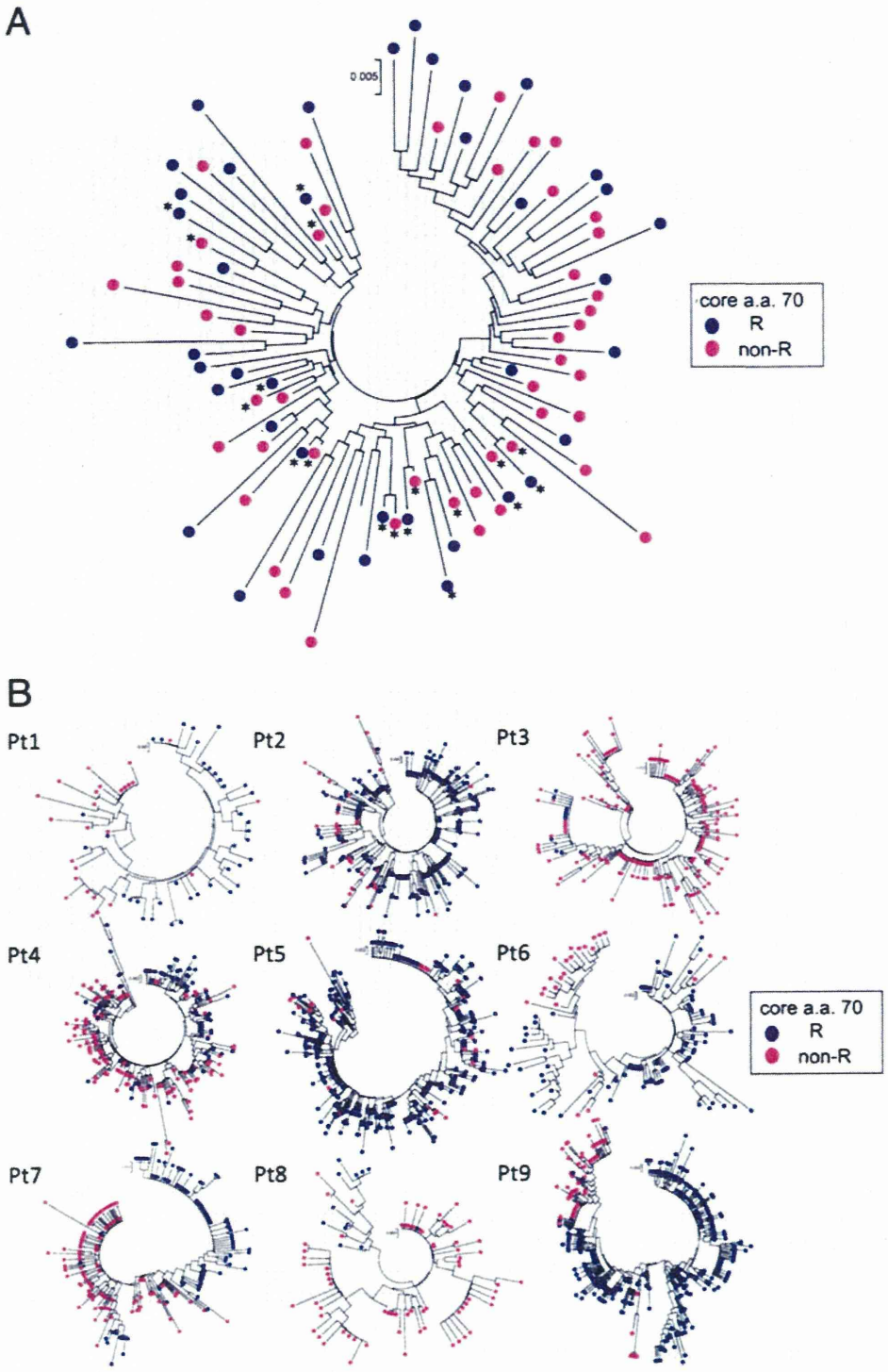

FIG 3 Phylogenetic trees were constructed using core sequences covering almost the entire core region. In the construction of those trees, the three bases of the core 70 codon were removed in the analysis of all 79 patients. Branches with core aa 70R are indicated by blue circles, while those with core aa 70non-R are indicated by pink circles. (A) Phylogenetic trees were constructed for all 79 patients by using dominant core sequences obtained from each patient. In the construction of the tree, two dominant sequences (a dominant core sequence in isolates with aa 70R and a dominant core sequence in isolates with aa 70non-R) were included in the analysis for each of the nine patients with high mixture rates (5% or more) of R and non-R at core aa 70 (Fig. 2A), while one dominant sequence each was included for other patients. (B) A phylogenetic tree of the core region was constructed for each patient with a high mixture rate (5% or more) of core aa 70R and core aa 70non-R. A total of nine patients were included in this analysis (patients 1 to 3 had CH; patients 4 to 7 had LC; and patients 9 and 10 had HCC). Pt, patient.

TABLE 5 Comparison of genetic distances among core subgroups related to aa 70 residues

Patient(s)[a]	Genetic distance (mean ± SD) between two core sequences[b]			Comparison of genetic distance measurements					
				Non-R–R vs non-R–non-R		Non-R–R vs R-R		Non-R–non-R vs R-R	
	Non-R–non-R	Non-R–R	R-R	Larger genetic distance	*P*	Larger genetic distance	*P*	Larger genetic distance	*P*
All (n = 79)	0.0349 ± 0.0101	0.0379 ± 0.0109	0.0401 ± 0.0113	Non-R–R	<0.001	R-R	<0.001	R-R	<0.001
CH									
Pt 1	0.0086 ± 0.0042	0.0098 ± 0.0037	0.0064 ± 0.0042	Non-R–R	<0.001	Non-R–R	<0.001	Non-R–non-R	<0.001
Pt 2	0.0097 ± 0.0048	0.0104 ± 0.0041	0.0087 ± 0.0038	Non-R–R	<0.001	Non-R–R	<0.001	Non-R–non-R	0.009
Pt 3	0.0107 ± 0.0058	0.0137 ± 0.0050	0.0034 ± 0.0022	Non-R–R	<0.001	Non-R–R	<0.001	Non-R–non-R	<0.001
LC									
Pt 4	0.0078 ± 0.0036	0.0103 ± 0.0038	0.0053 ± 0.0029	Non-R–R	<0.001	Non-R–R	<0.001	Non-R–non-R	<0.001
Pt 5	0.0118 ± 0.0090	0.0232 ± 0.0085	0.0159 ± 0.0170	Non-R–R	<0.001	Non-R–R	<0.001	No difference	0.991
Pt 6	0.0115 ± 0.0057	0.0121 ± 0.0055	0.0108 ± 0.0056	Non-R–R	<0.001	Non-R–R	<0.001	Non-R–non-R	<0.001
Pt 7	0.0141 ± 0.0085	0.0146 ± 0.0070	0.0136 ± 0.0067	Non-R–R	0.002	Non-R–R	<0.001	Non-R–non-R	<0.001
HCC									
Pt 8	0.0124 ± 0.0063	0.0225 ± 0.0060	0.0181 ± 0.0094	Non-R–R	<0.001	Non-R–R	<0.001	R-R	<0.001
Pt 9	0.0082 ± 0.0042	0.0162 ± 0.0047	0.0078 ± 0.0050	Non-R–R	<0.001	Non-R–R	<0.001	Non-R–non-R	<0.001

[a] Pt, patient.

[b] Non-R–non-R, comparison of two core sequences with residues other than R at aa 70; Non-R–R, comparison of a core sequence with a residue other than R at aa 70 and a core sequence with aa 70R; R-R, comparison of two core sequences with aa 70R. Genetic distances were calculated for all patients by using dominant sequences and for a single patient by using quasispecies sequences.

core sequence with aa 70R and a core sequence with aa 70non-R (non-R–R), demonstrating that core sequences with aa 70R were heterogeneous, while core sequences with aa 70non-R were homogeneous.

Next, to determine the association of the remainder of the core sequences in a single patient, phylogenetic trees were also constructed for each of the nine patients with high mixture rates (5% or more) of R and non-R residues at core aa 70 (Fig. 3B). As shown in Fig. 3B, HCV isolates with core aa 70R and those with core aa 70non-R formed distinctly clustered subgroups on the phylogenetic tree, according to the mutation status at core aa 70. Comparison of genetic distances also proved the finding that HCV isolates with core aa 70R and those with core aa 70non-R form distinctly clustered subgroups on the phylogenetic tree in a single patient, since genetic distances calculated between every two core sequences with aa 70R (R-R) or between every two core sequences with aa 70non-R (non-R–non-R) were significantly smaller than those between a core sequence with aa 70R and a core sequence with aa 70non-R (non-R–R). On the other hand, no significant difference was found when the genetic distance between two core sequences with aa 70non-R (non-R–non-R) and that between two core sequences with aa 70R (R-R) were compared in a single patient (Table 5).

Since the genetic relationships of the remainder of the core sequences were found to differ significantly according to the core aa 70 residue, we then investigated whether there are any common haplotypic sequences specific to each residue. In the comparison of dominant sequences in all 79 patients, most amino acid substitutions clustered in three amino acids (aa 70, aa 75, and aa 91) both in core sequences with aa 70R and in those with aa 70nonR, but no other substitutions specific to each core aa 70 residue were found (Fig. 4).

Quasispecies at core aa 70 and clinical characteristics. To clarify the association of the core aa 70 quasispecies with the clinical picture, levels of gamma-glutamyl transpeptidase (γ-GTP), albumin, platelets, and alpha-fetoprotein, as well as disease progression in the liver, were investigated for correlation with the core aa 70R/non-R mixture ratio. As shown in Fig. 5A and B, the values for these clinical parameters became significantly more abnormal as the proportion of non-R residues increased, showing that a high proportion of non-R residues at core aa 70 was significantly associated with disease severity and hepatocarcinogenesis.

DISCUSSION

This study examined, for the first time, the relationship between the progression of liver disease and the quasispecies nature of the HCV core region (already known to be associated with liver disease progression) by deep sequencing, with the focus on the core aa 70 residue. The analysis revealed that core aa 70 existed as a mixture of "mutant" Q/H (non-R) and "wild-type" R residues in most of the patients and that the proportion of mutant residues increased as liver disease advanced to LC and HCC. Meanwhile, phylogenetic analysis showed that the viral sequences of the almost-entire core region differed genetically depending on the status of core aa 70.

Before starting the analysis, we verified the rate of background error associated with the process of pyrosequencing by analyzing the control plasmid pCV-J4L6S (Fig. 1). Homopolymers of repeated bases, a weak point of pyrosequencing, were generated at two sites, with the same base appearing five and six times. The overall mutation rate at other sites was 0.092% ± 0.005%, and a mutation rate of 0.102% (mean + 2 SDs) or higher was defined as significant in the analysis, in order to avoid detecting background errors.

We focused our analysis on the quasispecies state of core aa 70,

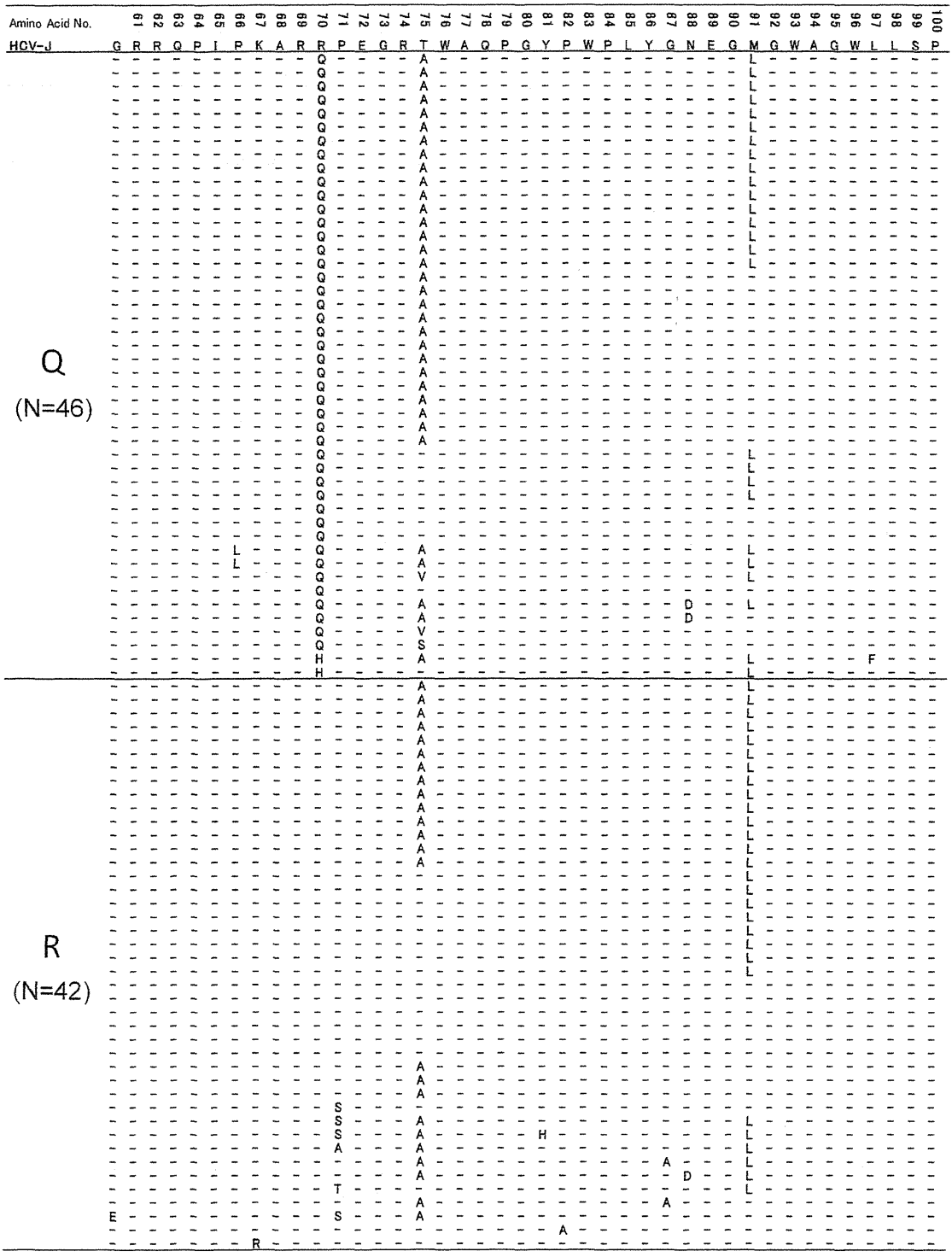

FIG 4 Dominant core amino acid haplotypic sequences dependent on the core aa 70 residues are given for all 79 patients. Two dominant sequences (a dominant core sequence in isolates with aa 70R and a dominant core sequence in isolates with aa 70non-R) were included for each of nine patients with high mixture rates (5% or more) of R and non-R at core aa 70, while one dominant sequence each was included for other patients. Therefore, a total of 88 haplotypic sequences are shown here. Since most amino acid mutations were observed in the limited core region, only that part of the core sequence is shown. The HCV-J isolate is used as the reference sequence for the core region.

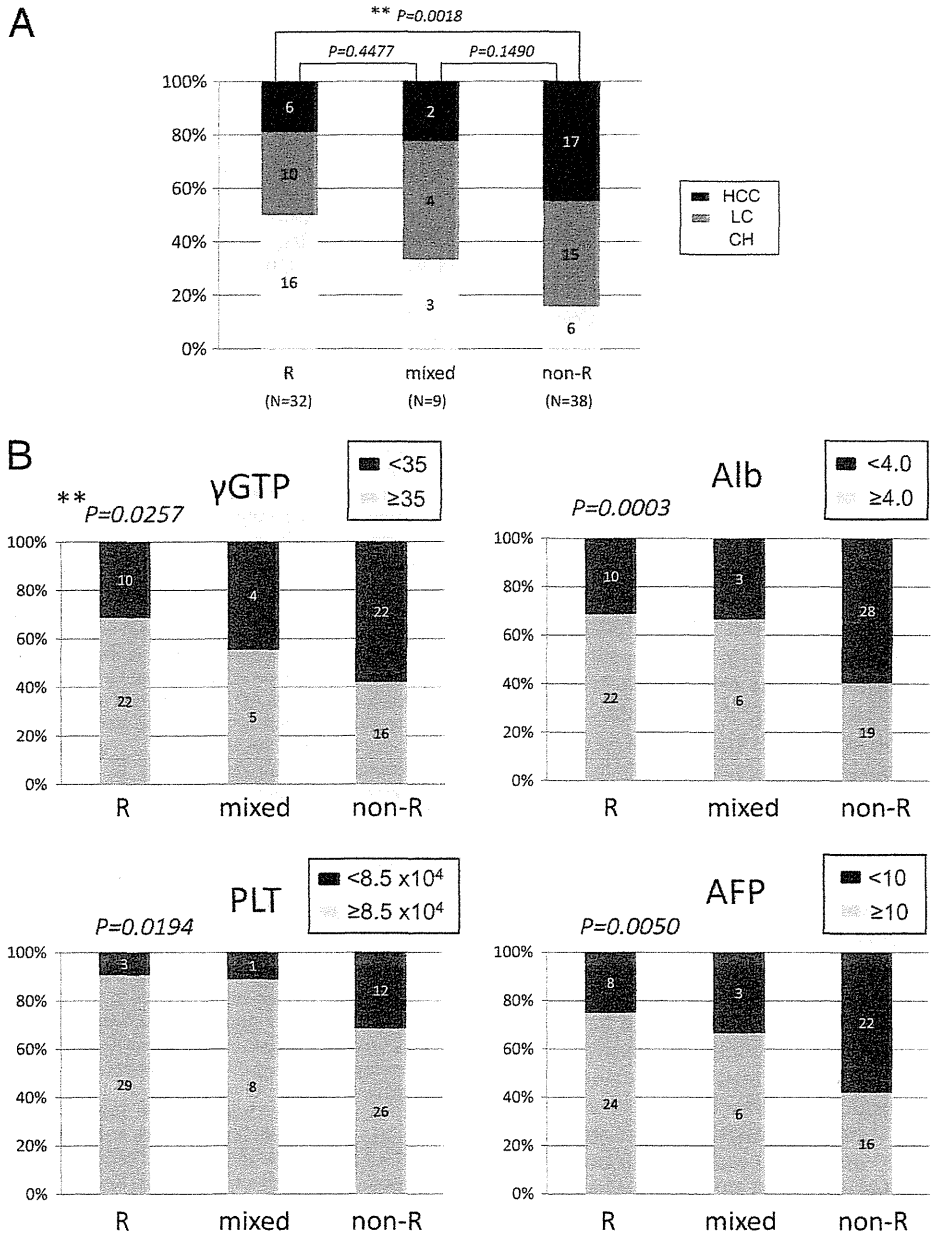

FIG 5 The advance of liver disease (A) and the levels of γ-GTP, albumin (Alb), platelets (PLT), and alpha-fetoprotein (AFP) (B) were investigated for correlation with the ratio of R to non-R at core aa 70. Results for R/R + non-R ratios of ≥95% (R), ≥5% and <95% (mixed), and <5% (non-R) are shown. **, Cochran-Armitage analysis.

because the presence of a quasispecies was expected at this position, considering reports by previous studies of its association with liver disease progression and the frequent observation of time-dependent changes (8, 9). R and non-R residues were mixed in 89.9% of the 79 patients examined in this study, indicating that the absence of a mixture was rare. Furthermore, the percentage of total isolates encoding non-R residues at this position showed a relationship with the advance of chronic liver disease, as shown in Fig. 2A and Table 3. Therefore, with regard to the relationship between the advance of liver disease and core aa 70, it may be accurate to say that a change in the ratio of amino acids at core aa 70, rather than mutation of core aa 70, was related to the advance of liver disease.

Because information for almost the entire core region was obtained from each patient, our next interest was to determine whether core aa 70 is associated with other viral regions. In other words, we sought to determine whether HCVs with core aa 70R and HCVs with core aa 70non-R are phylogenetically distinct variants. To clarify the issue, phylogenetic tree analysis using dominant sequences for the (almost-entire) core regions from all 79 patients was performed at first. This analysis disclosed, after the calculation of genetic distances, that core sequences with aa

70non-R were significantly more homogeneous than those with aa 70R, demonstrating that the hot spot core aa 70 residue is significantly associated with the remainder of the core sequence. Although the underlying mechanism is unclear, we speculated that the close correlation between core aa 70 residues and IL28B SNPs might have contributed to the result. That is, since endogenous IFN levels are known to be upregulated in patients with IL28B minor types (TG/GG) relative to those in patients with the IL28B major type (TT) in its natural state (28), it is possible that HCVs with core aa 70non-R, which are closely linked to IL28B TG/GG, are under strong antiviral pressure induced by IFN, resulting in the selection of more-homogeneous HCVs, which can survive in such an environment.

Considering this possibility, we proceeded to perform phylogenetic analyses of core sequences in single patients with high-percentage mixtures (5% or more) of R and non-R residues at core aa 70 by using deep-sequencing data, since the influence of endogenous IFNs was considered equal for all HCV isolates in a single patient. The deep-sequencing data showed that the genetic heterogeneity of core sequences in a single patient did not differ according to the core aa 70 residue but that core sequences formed distinct subgroups on the phylogenetic tree according to the core aa 70 residue (Fig. 3B), and this result was also proved by the calculation of genetic distances (Table 5). However, since no common haplotypic sequences specific to each residue at core aa 70 were found across the patients (Fig. 4), we cannot determine whether core aa 70R and aa 70non-R HCVs are phylogenetically distinct variants. It is possible that the result simply reflects a major evolutional event of core aa 70 mutations followed by derivative variants; however, extension of the investigation and analysis to viral regions beyond the core region might reveal such associations. However, due to the technical limitations of second-generation sequencers, deep-sequencing analysis of the long amplicon is difficult, and new technology is needed.

With regard to the mechanism underlying the relationship between the core protein and disease progression and hepatocarcinogenesis, a study using transgenic mice showed that the core protein induces HCC (29). Fat metabolism was accelerated in the liver, leading to inflammation, iron metabolism, oxidative stress, and insulin resistance, which were considered to be the carcinogenic factors (30–32). Clinically, mutation of the core and the concentration of γ-GTP in serum, a marker of steatosis, are related, and the relationship between IL28B SNP and liver steatosis or γ-GTP has been elucidated (33). In this study, moreover, we have confirmed the correlation between the core aa 70 mixture ratio, determined by deep-sequencing analysis, and clinical parameters reflecting disease progression, illustrating the significant association of core aa 70 with disease progression (Fig. 5A and B).

In conclusion, the quasispecies state of the core region was analyzed by deep sequencing. It was found that the status of the quasispecies was closely related to the advance of HCV-associated liver disease. In order to understand the mechanism of hepatocarcinogenesis, it is desirable to elucidate pathogenesis further by detailed examination of the quasispecies of the HCV core gene.

ACKNOWLEDGMENTS

Nobuyuki Enomoto received research funding from MSD (Tokyo, Japan) and Roche (Tokyo, Japan).

This study was supported in part by grants-in-aid from the Ministry of Education, Science, Sports and Culture of Japan (grants 23390195, 23791404, 24590964, and 24590965) and in part by grants-in-aid from the Ministry of Health, Labour, and Welfare of Japan (H23-kanen-001, H23-kanen-004, H23-kanen-006, H24-kanen-002, H24-kanen-004, and H25-kanen-006).

REFERENCES

1. Niederau C, Lange S, Heintges T, Erhardt A, Buschkamp M, Hurter D, Nawrocki M, Kruska L, Hensel F, Petry W, Haussinger D. 1998. Prognosis of chronic hepatitis C: results of a large, prospective cohort study. Hepatology 28:1687–1695.
2. Koike K. 2005. Molecular basis of hepatitis C virus-associated hepatocarcinogenesis: lessons from animal model studies. Clin. Gastroenterol. Hepatol. 3:S132–S135.
3. Akuta N, Suzuki F, Sezaki H, Suzuki Y, Hosaka T, Someya T, Kobayashi M, Saitoh S, Watahiki S, Sato J, Matsuda M, Arase Y, Ikeda K, Kumada H. 2005. Association of amino acid substitution pattern in core protein of hepatitis C virus genotype 1b high viral load and non-virological response to interferon-ribavirin combination therapy. Intervirology 48:372–380.
4. Akuta N, Suzuki F, Hirakawa M, Kawamura Y, Sezaki H, Suzuki Y, Hosaka T, Kobayashi M, Saitoh S, Arase Y, Ikeda K, Kumada H. 2011. Amino acid substitutions in hepatitis C virus core region predict hepatocarcinogenesis following eradication of HCV RNA by antiviral therapy. J. Med. Virol. 83:1016–1022.
5. Akuta N, Suzuki F, Kawamura Y, Yatsuji H, Sezaki H, Suzuki Y, Hosaka T, Kobayashi M, Arase Y, Ikeda K, Kumada H. 2007. Amino acid substitutions in the hepatitis C virus core region are the important predictor of hepatocarcinogenesis. Hepatology 46:1357–1364.
6. Fishman SL, Factor SH, Balestrieri C, Fan X, Dibisceglie AM, Desai SM, Benson G, Branch AD. 2009. Mutations in the hepatitis C virus core gene are associated with advanced liver disease and hepatocellular carcinoma. Clin. Cancer Res. 15:3205–3213.
7. Nakamoto S, Imazeki F, Fukai K, Fujiwara K, Arai M, Kanda T, Yonemitsu Y, Yokosuka O. 2010. Association between mutations in the core region of hepatitis C virus genotype 1 and hepatocellular carcinoma development. J. Hepatol. 52:72–78.
8. Akuta N, Suzuki F, Seko Y, Kawamura Y, Sezaki H, Suzuki Y, Hosaka T, Kobayashi M, Hara T, Saitoh S, Arase Y, Ikeda K, Kumada H. 2012. Complicated relationships of amino acid substitution in hepatitis C virus core region and IL28B genotype influencing hepatocarcinogenesis. Hepatology 56:2134–2141.
9. Miura M, Maekawa S, Kadokura M, Sueki R, Komase K, Shindo H, Ohmori T, Kanayama A, Shindo K, Amemiya F, Nakayama Y, Kitamura T, Uetake T, Inoue T, Sakamoto M, Okada S, Enomoto N. 2012. Analysis of viral amino acids sequences and the IL28B SNP influencing the development of hepatocellular carcinoma in chronic hepatitis C. Hepatol. Int. 6:386–396.
10. Ge D, Fellay J, Thompson AJ, Simon JS, Shianna KV, Urban TJ, Heinzen EL, Qiu P, Bertelsen AH, Muir AJ, Sulkowski M, McHutchison JG, Goldstein DB. 2009. Genetic variation in IL28B predicts hepatitis C treatment-induced viral clearance. Nature 461:399–401.
11. Rauch A, Kutalik Z, Descombes P, Cai T, Di Iulio J, Mueller T, Bochud M, Battegay M, Bernasconi E, Borovicka J, Colombo S, Cerny A, Dufour JF, Furrer H, Gunthard HF, Heim M, Hirschel B, Malinverni R, Moradpour D, Mullhaupt B, Witteck A, Beckmann JS, Berg T, Bergmann S, Negro F, Telenti A, Bochud PY. 2010. Genetic variation in *IL28B* is associated with chronic hepatitis C and treatment failure: a genome-wide association study. Gastroenterology 138:1338–1345.e7.
12. Suppiah V, Moldovan M, Ahlenstiel G, Berg T, Weltman M, Abate ML, Bassendine M, Spengler U, Dore GJ, Powell E, Riordan S, Sheridan D, Smedile A, Fragomeli V, Muller T, Bahlo M, Stewart GJ, Booth DR, George J. 2009. IL28B is associated with response to chronic hepatitis C interferon-alpha and ribavirin therapy. Nat. Genet. 41:1100–1104.
13. Tanaka Y, Nishida N, Sugiyama M, Kurosaki M, Matsuura K, Sakamoto N, Nakagawa M, Korenaga M, Hino K, Hige S, Ito Y, Mita E, Tanaka E, Mochida S, Murawaki Y, Honda M, Sakai A, Hiasa Y, Nishiguchi S, Koike A, Sakaida I, Imamura M, Ito K, Yano K, Masaki N, Sugauchi F, Izumi N, Tokunaga K, Mizokami M. 2009. Genome-wide association of IL28B with response to pegylated interferon-alpha and ribavirin therapy for chronic hepatitis C. Nat. Genet. 41:1105–1109.
14. Bochud PY, Bibert S, Kutalik Z, Patin E, Guergnon J, Nalpas B, Goossens N, Kuske L, Mullhaupt B, Gerlach T, Heim MH, Moradpour

D, Cerny A, Malinverni R, Regenass S, Dollenmaier G, Hirsch H, Martinetti G, Gorgiewski M, Bourliere M, Poynard T, Theodorou I, Abel L, Pol S, Dufour JF, Negro F. 2012. IL28B alleles associated with poor hepatitis C virus (HCV) clearance protect against inflammation and fibrosis in patients infected with non-1 HCV genotypes. Hepatology 55: 384–394.

15. Fabris C, Falleti E, Cussigh A, Bitetto D, Fontanini E, Bignulin S, Cmet S, Fornasiere E, Fumolo E, Fangazio S, Cerutti A, Minisini R, Pirisi M, Toniutto P. 2011. IL-28B rs12979860 C/T allele distribution in patients with liver cirrhosis: role in the course of chronic viral hepatitis and the development of HCC. J. Hepatol. 54:716–722.
16. Joshita S, Umemura T, Katsuyama Y, Ichikawa Y, Kimura T, Morita S, Kamijo A, Komatsu M, Ichijo T, Matsumoto A, Yoshizawa K, Kamijo N, Ota M, Tanaka E. 2012. Association of IL28B gene polymorphism with development of hepatocellular carcinoma in Japanese patients with chronic hepatitis C virus infection. Hum. Immunol. 73:298–300.
17. Marabita F, Aghemo A, De Nicola S, Rumi MG, Cheroni C, Scavelli R, Crimi M, Soffredini R, Abrignani S, De Francesco R, Colombo M. 2011. Genetic variation in the interleukin-28B gene is not associated with fibrosis progression in patients with chronic hepatitis C and known date of infection. Hepatology 54:1127–1134.
18. Pawlotsky JM. 2006. Hepatitis C virus population dynamics during infection. Curr. Top. Microbiol. Immunol. 299:261–284.
19. Hiraga N, Imamura M, Abe H, Hayes CN, Kono T, Onishi M, Tsuge M, Takahashi S, Ochi H, Iwao E, Kamiya N, Yamada I, Tateno C, Yoshizato K, Matsui H, Kanai A, Inaba T, Tanaka S, Chayama K. 2011. Rapid emergence of telaprevir resistant hepatitis C virus strain from wild-type clone in vivo. Hepatology 54:781–788.
20. Nasu A, Marusawa H, Ueda Y, Nishijima N, Takahashi K, Osaki Y, Yamashita Y, Inokuma T, Tamada T, Fujiwara T, Sato F, Shimizu K, Chiba T. 2011. Genetic heterogeneity of hepatitis C virus in association with antiviral therapy determined by ultra-deep sequencing. PLoS One 6:e24907. doi:10.1371/journal.pone.0024907.
21. Verbinnen T, Van Marck H, Vandenbroucke I, Vijgen L, Claes M, Lin TI, Simmen K, Neyts J, Fanning G, Lenz O. 2010. Tracking the evolution of multiple *in vitro* hepatitis C virus replicon variants under protease inhibitor selection pressure by 454 deep sequencing. J. Virol. 84:11124–11133.
22. Wang GP, Sherrill-Mix SA, Chang KM, Quince C, Bushman FD. 2010. Hepatitis C virus transmission bottlenecks analyzed by deep sequencing. J. Virol. 84:6218–6228.
23. Nagayama K, Kurosaki M, Enomoto N, Maekawa SY, Miyasaka Y, Tazawa J, Izumi N, Marumo F, Sato C. 1999. Time-related changes in full-length hepatitis C virus sequences and hepatitis activity. Virology 263: 244–253.
24. Gates AT, Sarisky RT, Gu B. 2004. Sequence requirements for the development of a chimeric HCV replicon system. Virus Res. 100:213–222.
25. Tamura K, Peterson D, Peterson N, Stecher G, Nei M, Kumar S. 2011. MEGA5: molecular evolutionary genetics analysis using maximum likelihood, evolutionary distance, and maximum parsimony methods. Mol. Biol. Evol. 28:2731–2739.
26. Becker EA, Burns CM, Leon EJ, Rajabojan S, Friedman R, Friedrich TC, O'Connor SL, Hughes AL. 2012. Experimental analysis of sources of error in evolutionary studies based on Roche/454 pyrosequencing of viral genomes. Genome Biol. Evol. 4:457–465.
27. Quince C, Lanzen A, Curtis TP, Davenport RJ, Hall N, Head IM, Read LF, Sloan WT. 2009. Accurate determination of microbial diversity from 454 pyrosequencing data. Nat. Methods 6:639–641.
28. Honda M, Sakai A, Yamashita T, Nakamoto Y, Mizukoshi E, Sakai Y, Nakamura M, Shirasaki T, Horimoto K, Tanaka Y, Tokunaga K, Mizokami M, Kaneko S. 2010. Hepatic ISG expression is associated with genetic variation in interleukin 28B and the outcome of IFN therapy for chronic hepatitis C. Gastroenterology 139:499–509.
29. Moriya K, Fujie H, Shintani Y, Yotsuyanagi H, Tsutsumi T, Ishibashi K, Matsuura Y, Kimura S, Miyamura T, Koike K. 1998. The core protein of hepatitis C virus induces hepatocellular carcinoma in transgenic mice. Nat. Med. 4:1065–1067.
30. Leandro G, Mangia A, Hui J, Fabris P, Rubbia-Brandt L, Colloredo G, Adinolfi LE, Asselah T, Jonsson JR, Smedile A, Terrault N, Pazienza V, Giordani MT, Giostra E, Sonzogni A, Ruggiero G, Marcellin P, Powell EE, George J, Negro F. 2006. Relationship between steatosis, inflammation, and fibrosis in chronic hepatitis C: a meta-analysis of individual patient data. Gastroenterology 130:1636–1642.
31. Nishina S, Hino K, Korenaga M, Vecchi C, Pietrangelo A, Mizukami Y, Furutani T, Sakai A, Okuda M, Hidaka I, Okita K, Sakaida I. 2008. Hepatitis C virus-induced reactive oxygen species raise hepatic iron level in mice by reducing hepcidin transcription. Gastroenterology 134:226–238.
32. Okuda M, Li K, Beard MR, Showalter LA, Scholle F, Lemon SM, Weinman SA. 2002. Mitochondrial injury, oxidative stress, and antioxidant gene expression are induced by hepatitis C virus core protein. Gastroenterology 122:366–375.
33. Abe H, Ochi H, Maekawa T, Hayes CN, Tsuge M, Miki D, Mitsui F, Hiraga N, Imamura M, Takahashi S, Ohishi W, Arihiro K, Kubo M, Nakamura Y, Chayama K. 2010. Common variation of IL28 affects γ-GTP levels and inflammation of the liver in chronically infected hepatitis C virus patients. J. Hepatol. 53:439–443.

JOURNAL OF VIRAL HEPATITIS JVH

Journal of Viral Hepatitis, 2012 doi:10.1111/j.1365-2893.2012.01649.x

IL-28B (IFN-λ3) and IFN-α synergistically inhibit HCV replication

H. Shindo,[1] S. Maekawa,[1] K. Komase,[1] M. Miura,[1] M. Kadokura,[1] R. Sueki,[1] N. Komatsu,[1] K. Shindo,[1] F. Amemiya,[1] Y. Nakayama,[1] T. Inoue,[1] M. Sakamoto,[1] A. Yamashita,[2] K. Moriishi[2] and N. Enomoto[1] [1]*First Department of Internal Medicine, University of Yamanashi, Yamanashi, Japan; and* [2]*Department of Microbiology, University of Yamanashi, Yamanashi, Japan*

Received March 2012; accepted for publication June 2012

SUMMARY. Genetic variation in the IL-28B (interleukin-28B; interferon lambda 3) region has been associated with sustained virological response (SVR) rates in patients with chronic hepatitis C treated with peginterferon-α and ribavirin. However, the mechanisms by which polymorphisms in the IL-28B gene region affect host antiviral responses are not well understood. Using the HCV 1b and 2a replicon system, we compared the effects of IFN-λs and IFN-α on HCV RNA replication. The anti-HCV effect of IFN-λ3 and IFN-α in combination was also assessed. Changes in gene expression induced by IFN-λ3 and IFN-α were compared using cDNA microarray analysis. IFN-λs at concentrations of 1 ng/mL or more exhibited concentration- and time-dependent HCV inhibition. In combination, IFN-λ3 and IFN-α had a synergistic anti-HCV effect; however, no synergistic enhancement was observed for interferon-stimulated response element (ISRE) activity or upregulation of interferon-stimulated genes (ISGs). With respect to the time course of ISG upregulation, the peak of IFN-λ3-induced gene expression occurred later and lasted longer than that induced by IFN-α. In addition, although the genes upregulated by IFN-α and IFN-λ3 were similar to microarray analysis, interferon-stimulated gene expression appeared early and was prolonged by combined administration of these two IFNs. In conclusion, IFN-α and IFN-λ3 in combination showed synergistic anti-HCV activity *in vitro*. Differences in time-dependent upregulation of these genes might contribute to the synergistic antiviral activity.

Keywords: HCV, IFN-λ, IL-28B, ISG, synergistic inhibition, microarray.

INTRODUCTION

In 2009, reports from three genome-wide association studies revealed that several single-nucleotide polymorphisms (SNPs) (rs12979860, rs12980275 and rs8099917) around the IL-28B (interleukin-28B; interferon lambda 3) gene are strongly associated with sustained viral response (SVR) to PEG-IFN and RBV treatment for chronic hepatitis C [1–3]. Specifically, patients with the TG or GG genotype at rs8099917 infected with genotype 1b are more resistant to PEG-IFN and RBV treatment than patients with the TT genotype. IL-28B haplotypes were also reported to be strongly associated with spontaneous HCV clearance [1, 4, 5].

IL-28B is a member of the type III IFN family [6], consisting of IFN-λ1 (IL-29), IFN-λ2 (IL-28A) and IFN-λ3 (IL-28B). IFN-λs bind to their cognate receptor, composed of IL28R1 and IL10R2, and then activate the receptor-associated Janus-activated kinases (Jak) 1 and tyrosine kinase (Tyk) 2, leading to the activation of downstream signal transducer and activator of transcription (STAT) proteins, STAT1 and STAT2. Similar to type I IFN signalling, the Jak-STAT signalling pathway activates the IFN-stimulated response element (ISRE) within the promoter region of interferon-stimulated genes (ISGs) [7].

Concerning the functional role of IL-28B in HCV infection, two of *in vivo* studies assessed the correlation of IL-28A/B mRNA levels in whole blood and peripheral blood mononuclear cells (PBMC) with IL-28B haplotypes at position rs8099917. IL-28A mRNA and IL-28B mRNA levels in subjects with the TT genotype were higher than in subjects with other genotypes (TG or GG), suggesting an association between higher amounts of endogenous IFN-λs and HCV clearance [2, 3]. On the other hand, subjects

Abbreviations: DMEM, Dulbecco's modified Eagle's medium; FBS, foetal bovine serum; ISG, interferon-stimulated genes; MTS, dimethylthiazol carboxymethoxyphenyl sulphophenyl tetrazolium; PBMC, peripheral blood mononuclear cells; SNP, single-nucleotide polymorphisms; STAT, signal transducer and activator of transcription; SVR, sustained viral response.

Correspondence: Shinya Maekawa, M.D., Ph.D., First Department of Internal Medicine, University of Yamanashi, 1110, Shimokato, Chuo, Yamanashi 409-3898, Japan. E-mail: maekawa@yamanashi.ac.jp